frontiers | Frontiers in Materials

TYPE Original Research
PUBLISHED 30 July 2025
DOI 10.3389/fmats.2025.1614951

OPEN ACCESS

EDITED BY
John L. Provis,
Paul Scherrer Institut (PSI), Switzerland

REVIEWED BY
Lucio Nobile,
University of Bologna, Italy
Congjie Wei,
Texas A and M University, United States

*CORRESPONDENCE
Tianbo Peng,
ptb@tongji.edu.cn
Muhammad Mubashir Ajmal,
mubashir.ajmal@uos.edu.pk

RECEIVED 20 April 2025
ACCEPTED 18 July 2025
PUBLISHED 30 July 2025

CITATION
Akhlaq H, Peng T, Ajmal MM, Khan MS and Riaz M (2025) Impact of GGBS on the rheology and mechanical behavior of pumpable concrete.
Front. Mater. 12:1614951.
doi: 10.3389/fmats.2025.1614951

Impact of GGBS on the rheology and mechanical behavior of pumpable concrete

Hanzlah Akhlaq[1,2], Tianbo Peng[1,3]*, Muhammad Mubashir Ajmal[2]*, Muhammad Salman Khan[1] and Mamoon Riaz[4]

[1]College of Civil Engineering, Tongji University, Shanghai, China, [2]College of Engineering and Technology, University of Sargodha, Sargodha, Pakistan, [3]State Key Laboratory of Disaster Reduction in Civil Engineering, Tongji University, Shanghai, China, [4]Department of Civil Engineering, International Islamic University, Islamabad, Pakistan

The increasing demand for high-performance pumpable concrete in large-scale infrastructure projects necessitates optimizing workability and strength while reducing environmental impact. This research explores the rheological, workability, and mechanical behavior of pumpable concrete with fractional substitution of cement by Ground Granulated Blast Furnace Slag (GGBS), aiming to enhance sustainability and performance. A total of 30 mix designs with GGBS replacements ranging from 0% to 90% were prepared, systematically optimizing the water-binder ratio (W/B) and superplasticizer dosage to maintain constant workability (i.e., 130 ± 15 mm slump value) to achieve the required pumpability. A total of 810 samples were prepared and tested to evaluate compressive strength (450 specimens at 7, 14, 21, 28, and 56 days), splitting tensile strength (180 specimens at 28 and 56 days), and flexural strength (180 specimens at 28 and 56 days). The findings show that GGBS enhances the rheological behavior of fresh concrete by lowering both plastic viscosity and yield stress, which in turn improves its flowability and pumpability. The optimal GGBS replacement level was found to be in the range of 30%–50%, where the best balance between workability and strength development was achieved. Compressive strength tests showed that while higher GGBS levels resulted in delayed early-age strength gain, long-term strength development was significantly enhanced due to pozzolanic reactions. The splitting tensile and flexural strength results followed similar trends, demonstrating optimal performance at 40% GGBS replacement. This study confirms that the controlled use of GGBS in pumpable concrete enhances both fresh and hardened properties while promoting sustainability by reducing OPC consumption and associated carbon emissions. The findings provide valuable insights for optimizing mix designs to achieve high-performance, eco-friendly pumpable concrete suitable for modern construction applications.

KEYWORDS

GGBS, pumpable concrete, constant slump concrete, environmental protection, sustainability, Rheological properties

1 Introduction

Modern construction techniques demand materials that can meet the challenges of large-scale and complex projects, such as high-rise buildings, long-span bridges, deep tunnels, etc. (Basit et al., 2024; Akhlaq et al., 2022; Akhlaq et al., 2025a). Among these, pumpable concrete has become indispensable due to its ability to flow smoothly through pipelines to reach otherwise inaccessible locations. Its ease of placement, reduced labor requirements, and enhanced construction speed make it a preferred choice for many structural applications (Yuan et al., 2022).

Pumpability in concrete technology refers to the ability of a concrete mixture to flow through a pipeline without significant loss of quality. It is not an inherent property of concrete but rather the outcome of optimizing the concrete mix design, pipeline geometry, and pumping equipment (Kaplan et al., 2005). The pumpability of concrete is highly dependent on its rheological characteristics, particularly plastic viscosity and yield stress, which govern flow behavior. Plastic viscosity describes the resistance of a material to continued flow after movement has commenced, whereas yield stress refers to the minimum stress needed to start the flow (Banfill, 1990). For effective pumping, concrete must exhibit low yield stress to start flowing easily and moderate plastic viscosity to maintain steady flow without segregation (Feys et al., 2016). Achieving optimal rheological behavior involves more than just mix design. The use of chemical admixtures, such as superplasticizers, enhances flowability and reduces water demand without compromising cohesion (Paritala et al., 2023). Proper rheological control ensures that the concrete flows smoothly through pipelines, preventing issues like segregation, bleeding, or blockages during extended pumping operations (Binns, 2003).

Despite the practical benefits of pumpable concrete, its environmental implications remain a concern. Ordinary Portland Cement (OPC) manufacturing is a major source of worldwide CO_2 emissions, contributing roughly 5%–8% to the total (Ajmal et al., 2023; Khan et al., 2025). This environmental burden is largely due to the energy-intensive nature of cement manufacturing and the release of carbon dioxide during limestone calcination (Stanmore and Gilot, 2005). To alleviate the environmental bearing of cement manufacturing, the incorporation of supplementary cementitious materials (SCMs) has become increasingly popular (Riaz et al., 2022). These materials not only contribute to a reduction in CO_2 emissions but also increase the strength and durability of concrete (Malhotra, 2000). Commonly used SCMs include industrial waste such as fly ash, silica fume, and ground granulated blast furnace slag (GGBS). Among them, GGBS is particularly notable for its effectiveness in enhancing performance characteristics of concrete while substantially lowering its environmental footprint (Suresh and Nagaraju, 2015). GGBS is a secondary material derived as a waste by-product from the iron-making process in blast furnaces. If not reused, GGBS disposal poses significant environmental challenges, including landfill use and potential soil and water contamination. By incorporating GGBS in concrete, its disposal issue as industrial waste can be addressed, contributing to a circular economy and sustainable construction practices.

Gee (1979), Roy (1982), Wan et al. (2004) indicate that the incorporation of GGBS markedly improves the compressive strength of concrete. This increase is essentially attributed to its pozzolanic behavior and the consequent densification of the cementitious matrix. Incorporating GGBS into concrete reduces the heat of hydration, enhances resistance to chloride and sulfate attacks, and decreases permeability, making it ideal for aggressive environments (Nadir and Ahmed, 2022). In addition to its durability benefits, GGBS improves the workability and cohesiveness of fresh concrete, making it particularly advantageous for pumpable applications (Akhlaq et al., 2025b; Alkuhly, 2021).

Although numerous studies have explored the benefits of GGBS in conventional concrete, its application in pumpable concrete, particularly at high replacement levels, remains under-researched. The collective impact of GGBS and superplasticizers on the rheological and mechanical behavior of pumpable concrete has yet to be comprehensively analyzed. Furthermore, there is a lack of clear guidelines for optimizing mix designs to achieve pumpable concrete. This research seeks to bridge these gaps by investigating the influence of partial substitution of cement with GGBS on the performance of pumpable concrete. The primary objective is to assess the rheological behavior of fresh concrete, specifically yield stress and plastic viscosity, as well as the mechanical behavior of hardened concrete, including compressive, splitting tensile, and flexural strengths. Moreover, the study investigates the mix design of pumpable concrete by adjusting GGBS replacement levels and superplasticizer dosages to optimize the balance between workability and strength.

2 Research significance

This research holds substantial promises for advancing both the technical and environmental dimensions of concrete production. By demonstrating the viability of GGBS-based pumpable concrete, the study not only addresses the pressing need to decrease Ordinary Portland Cement (OPC) consumption, a major contributor to global CO_2 emissions, but also provides a practical approach to repurposing an industrial by-product that would otherwise pose environmental disposal challenges. Focusing on rheological properties like yield stress and plastic viscosity, this work supplies much-needed insight into how GGBS and superplasticizers synergistically enhance pumpability and overall performance, especially under high-volume replacement conditions where current literature remains sparse. Moreover, the findings are expected to yield clear guidelines for mix design optimization, enabling practitioners to balance sustainability, cost-effectiveness, and structural performance. Ultimately, this study's integrated approach, spanning rheology, mechanical strength, and environmental impact, marks a step forward in fostering a more sustainable construction industry while extending the frontiers of knowledge on pumpable concrete systems.

3 Experimental program

3.1 Materials

This study utilized several key materials to produce and evaluate pumpable concrete with varying levels of GGBS as a partial replacement for OPC. OPC conforming to ASTM C150 (A. ASTM C150, 2017) was used as the primary binder in all

TABLE 1 Chemical analysis of binding materials.

Binder	Chemical composition (%)								LOI[a]
	SiO_2	CaO	MgO	Al_2O_3	Fe_2O_3	K_2O	Na_2O	SO_3	
Cement	20.87	61.11	1.42	5.04	3.11	0.54	0.23	2.44	2.88
GGBS	38.19	31.92	8.75	11.18	1.88	0.41	1.26	-	1.1

[a]Loss on ignition.

TABLE 2 Physical parameters of binders.

Physical properties	Cement	GGBS
Specific Gravity (g/cm^3)	3.15	2.9
Specific Surface (cm^2/g)	3560	4050
Initial Setting Time (min)	82	
Final Setting Time (min)	182	

concrete mixtures. The setting times were evaluated as per ASTM C191 (ASTMC191-08, 2009), with an initial setting time of 82 min and a final setting time of 182 min, ensuring compliance with standards for pumpable concrete. The chemical analysis and physical characteristics of cement are given in Tables 1, 2.

The GGBS complied with ASTM C989 (ASTM C989, 2004) and was classified as Grade 100, often used in high-strength or performance-oriented concrete. The Pozzolanic Activity Index and Strength Activity Index, measured as per ASTM C311 (ASTM-C311-11, 2019) and ASTM C989 (ASTM C989, 2004), were 75% and 85% at 28 days, respectively. These properties highlight the suitability of GGBS for producing durable and sustainable pumpable concrete. The chemical analysis and physical characteristics of GGBS are provided in Tables 1, 2.

Locally available river sand was utilized as the fine aggregate in this research with a fineness modulus of 2.75. To ensure quality, the sand was washed and sieved to eliminate impurities and oversized particles, in accordance with ASTM C136 (ASTM International, 2019). Course aggregate from local crusher was utilized in the experimental work, with a particle size not exceeding 19 mm. Key physical properties, including a specific gravity of 2.70 (g/cm^3) and a water absorption of 0.8%, were tested as per ASTM C127 (ASTM C127, 2001). Sieve analysis ensured proper gradation, essential for achieving pumpability and durability. To attain the required workability for pumpable concrete, a water-reducing admixture conforming to ASTM C494 (ASTM C494, 2005) Type F specifications was utilized.

3.2 Mix proportions

In total, 30 concrete mixtures were prepared, including three control mixes containing only OPC (A1, B1, & C1) and twenty-seven mixtures incorporating GGBS with varying replacement levels (10%, 20%, …, 90%). These mixes were grouped into three series (A, B, and C) based on nominal ratio-based mix designs, a common practice in local construction (e.g., 1:1:2, 1:2:4, etc.). Specifically, Series A used a 1:1:2 ratio of coarse aggregate: fine aggregate: cement, Series B used a 1:2:4 ratio, and Series C used a 1:3:6 ratio. By selecting these three mixes, the study captures a representative range of paste contents, spanning from a relatively rich mix (Series A) to moderate (Series B) and lean (Series C), thereby reflecting typical local practice and ensuring broad applicability of the findings.

The pumpable concrete mixes were initially designed following ACI 211-1 (Standard, 1996). The final mix proportions were determined after multiple trials to achieve a consistent slump of 130 ± 15 mm (Rumman, 2018) for three mix series incorporating GGBS.

The initial mix design was developed with a fixed water-to-binder (w/b) ratio of 0.47 and a superplasticizer (SP) dosage of 1.5% by weight of the total binder. The SP was thoroughly mixed with the total design water volume. To adjust workability and meet the target slump (130 ± 15 mm), the SP-water solution was gradually introduced during mixing. The process began by adding 60% of the solution, with slump measured after each incremental addition. The point at which the desired slump was achieved marked the final quantity of solution added.

Based on the volume of solution actually used, the final w/b ratio and SP dosage (% of binder weight) were back-calculated for each mix. Although both values varied across mixes, the ratio of w/b to SP dosage was consistently maintained at 31.3 for all specimens. For instance, in Mix A5, the target slump was achieved at 61.7% solution addition, resulting in a w/b ratio of 0.29 and SP dosage of 0.926%. In contrast, Mix C1 required 100% of the solution, yielding a w/b ratio of 0.47 and SP dosage of 1.5%. In both cases, the w/b-to-SP dosage ratio remained constant at 31.3.

The slump test, conducted in accordance with ASTM C143 (ASTM C143/C143M, 2015), was used to assess the workability of fresh concrete, with the associated mix proportions provided in Table 3.

3.3 Preparation of samples and tests carried out

The study involved the preparation of 810 specimens to assess mechanical properties. All specimens were prepared in accordance with standard procedures outlined in (Documents and Information, 2005). Immediately after casting, the molds were sealed with polythene sheets to minimize moisture evaporation and were kept in a laboratory environment maintained at 20°C ± 1°C. The specimens

10.3389/fmats.2025.1614951

TABLE 3 Mix design of pumpable concrete.

Mix ID	% GGBS	Adjusted W/B Ratio	Adjusted SP Dosage (% of Binder)
A1 (1:1:2)	0	0.40	1.28%
A2 (1:1:2)	10	0.35	1.12%
A3 (1:1:2)	20	0.34	1.07%
A4 (1:1:2)	30	0.30	0.96%
A5 (1:1:2)	40	0.29	0.93%
A6 (1:1:2)	50	0.32	1.02%
A7 (1:1:2)	60	0.34	1.09%
A8 (1:1:2)	70	0.36	1.15%
A9 (1:1:2)	80	0.37	1.18%
A10 (1:1:2)	90	0.38	1.20%
B1 (1:2:4)	0	0.42	1.34%
B2 (1:2:4)	10	0.40	1.28%
B3 (1:2:4)	20	0.37	1.18%
B4 (1:2:4)	30	0.34	1.09%
B5 (1:2:4)	40	0.33	1.06%
B6 (1:2:4)	50	0.31	1.00%
B7 (1:2:4)	60	0.33	1.04%
B8 (1:2:4)	70	0.35	1.10%
B9 (1:2:4)	80	0.35	1.12%
B10 (1:2:4)	90	0.36	1.15%
C1 (1:3:6)	0	0.47	1.50%
C2 (1:3:6)	10	0.43	1.37%
C3 (1:3:6)	20	0.41	1.30%
C4 (1:3:6)	30	0.39	1.24%
C5 (1:3:6)	40	0.36	1.15%
C6 (1:3:6)	50	0.34	1.09%
C7 (1:3:6)	60	0.35	1.13%
C8 (1:3:6)	70	0.37	1.18%
C9 (1:3:6)	80	0.38	1.22%
C10 (1:3:6)	90	0.39	1.24%

were demolded after 24 h and submersed in water, also maintained at 20°C ± 1°C, where they remained until their respective testing ages.

3.3.1 Consistency

The standard consistency of cement paste was determined via Vicat apparatus in line with ASTM C187 (Astm, 2004) for different levels of GGBS replacement (0%–90%).

3.3.2 Setting time

Initial and final setting times were determined following the procedures outlined in ASTM C191 (International, 2008). The initial setting time was assessed using a 1 mm square needle, with measurements taken until the penetration depth reached 5 ± 0.5 mm from the base of the mold. The final setting time was assessed with an annular attachment, taking measurements every 30 min until the paste surface showed no visible indentation.

3.3.3 Workability

Concrete workability was evaluated through the slump test, conducted immediately after mixing and in accordance with ASTM C143 (ASTM, 2014). The slump was maintained within the specified range to ensure pumpability.

3.3.4 Rheological properties

The rheological behavior of each concrete mix was assessed using a state-of-the-art rheometer equipped with a four-blade vane, measuring 50.1 mm in length and 15.3 mm in diameter. The sample volume was selected to approximate an infinite medium, ensuring reliable measurement conditions (Nguyen and V Boger, 1992). To maintain consistency, the concrete paste was manually remixed before testing to prevent particle settlement and ensure homogeneity. A 30-second resting period was followed to allow the dissipation of residual stresses induced during mixing.

All fresh concrete and mortar samples were tested at approximately 15 min after the mixing water was introduced. To minimize any thixotropic effects or early structural buildup, we began each test with a 30-second high-speed shearing phase (Roussel, 2006). Next, the rotational speed of the rheometer was decreased stepwise over 0.6 rev/s to 0.1 rev/s range, corresponding to a maximum shear rate of about 10 s^{-1}. Each speed step included a 2-second transition followed by a 3-second measurement period to allow the system to reach near steady-state conditions. Following these measurements, the Bingham model was employed to analyze the data and extract values for yield stress and plastic viscosity (Feys et al., 2007).

To validate the applicability of the Bingham model for analyzing the rheological behavior of the concrete mixes, experimental shear stress versus shear rate data were plotted alongside model predictions. As shown in Figure 1, the data for mixtures A6, B6, and C6 closely follow linear trends, indicating a strong fit with the Bingham model. This supports the model's assumption of a linear relationship between shear stress and shear rate for cementitious systems with varying GGBS contents. The consistency of the linear fits across mix types with different aggregate proportions (1:1:2,

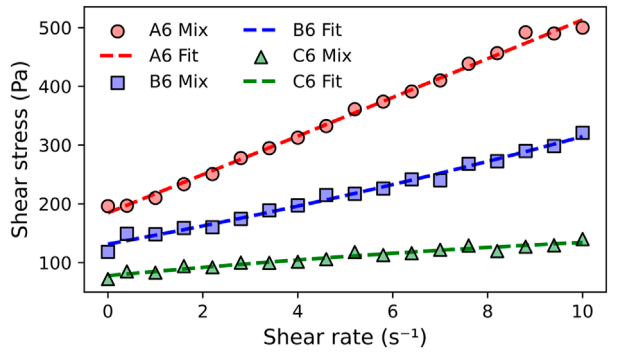

FIGURE 1
Rheological behavior of fresh concrete mixtures fitted with the bingham model.

TABLE 4 Summary of tests for paste and fresh concrete properties.

Test name	ASTM standard	Remarks
Consistency	ASTM C187 (Astm, 2004)	Cement-GGBS Paste
Setting Time	ASTM C191 (International, 2008)	Cement-GGBS Paste
Workability	ASTM C143 (ASTM, 2014)	Fresh Concrete
Yield Stress	ASTM C1749 (ASTM International, 2025)	Fresh Concrete
Plastic Viscosity		Fresh Concrete

1:2:4, and 1:3:6) further reinforces the appropriateness of using the Bingham model in this study (Park et al., 2005).

3.3.5 Mechanical properties

Compressive strength was evaluated by calculating the average crushing strength of three cylindrical specimens for each mix, tested at 7, 14, 21, 28, and 56 days. The splitting tensile and flexural strengths were determined using the mean values of three cylinders and prisms, tested at 28 and 56 days.

A summary of the different tests conducted on paste and fresh concrete is presented in Table 4, while the tests for hardened concrete specimens are detailed in Table 5.

4 Results and discussion

4.1 Properties of cement paste with GGBS

4.1.1 Consistency

The normal consistency of cement paste was measured for different levels of GGBS replacement, ranging from 0% to 90%, with the results shown in Figure 2. The values of water required for normal consistency exhibited an incremental trend as the percentage of GGBS replacement increased. For pure cement paste (0% GGBS), the consistency was measured as 23%, which increased gradually to 30.1% at 90% GGBS replacement. GGBS contributes to higher consistency values primarily due to its physical and chemical properties. The smoother and glassy texture and reduced friction of GGBS particles enhance the paste's cohesiveness, which requires more water to achieve the standard flow (Siddique and Bennacer, 2012). Furthermore, the higher fineness of GGBS contributes to an increased specific surface area, leading to greater water retention in the paste. The consistency values of 28% at 50% GGBS replacement and 31.1% at 90% GGBS replacement suggest that GGBS enhances the paste's plasticity while maintaining its stability. A linear regression of the data points yielded the best-fit line $y = 0.080x+23.38$, as shown in Figure 2, with a high coefficient of determination ($R^2 = 0.98$). This strong correlation confirms a near-linear relationship between the GGBS replacement level and the paste consistency.

4.1.2 Initial and final setting time

The setting times of cement paste serve as key indicators of the hydration process and are notably affected by the partial substitution of cement with GGBS. The initial setting time indicates when the paste begins to lose its plasticity, whereas the final setting time signifies when it has hardened enough to withstand defined pressure levels. These parameters are particularly important in evaluating the suitability of GGBS-blended cement paste for practical construction applications, especially for pumpable concrete.

The results, presented in Figure 3, show a progressive increase in both the initial and final setting times as the percentage of GGBS replacement increased (Mark et al., 2019). For 100% OPC (0% GGBS), the initial setting time was recorded at 82 min, and the final setting time at 182 min. As the GGBS replacement level increased to 90%, the initial and final setting times extended significantly to 192 min and 298 min, respectively.

This pattern aligns with the observations of Yu et al., who attributed the extended setting times to the slower hydration kinetics associated with GGBS (Yu et al., 2021). GGBS, being a latent hydraulic material, relies on the activation provided by OPC and water to contribute to hydration. As the OPC content decreases with higher GGBS replacement, the availability of active hydration compounds, such as tri-calcium silicate (C_3S), diminishes, leading to slower setting (Liew et al., 2024).

Additionally, the fineness of GGBS, combined with its smoother surface texture, reduces its immediate reactivity compared to OPC. This delayed reaction is particularly evident in the slower initial hydration phase, which is critical for the development of early strength. However, the extended setting times also offer some practical advantages. The decrease in heat of hydration observed with increased GGBS content helps reduce the risk of thermal cracking in large-scale concrete elements, thereby making GGBS-based binders well-suited for mass concrete applications (Lawrence et al., 2012).

The findings also indicate a consistent rise in final setting time as the GGBS content increases. Specifically, the final setting time extended by around 63%, increasing from 182 min at 0% GGBS to 298 min at 90% replacement. However, at high GGBS levels, delayed setting may become a challenge for rapid construction schedules, particularly in cold climates where hydration is naturally slowed. Moreover, linear regressions of the data indicate a near-linear trend: for the initial setting time, $y = 1.192x+75.18$ with $R^2 = 0.9544$, and for the final setting time, $y = 1.234x+170.67$ with $R^2 = 0.9245$. These high coefficients of determination confirm a strong correlation

TABLE 5 Summary of test methods for hardened concrete properties.

Test name	ASTM standard	Specimen	Specimen size	Remarks
Compressive Strength	ASTM C39 (ASTM: C39/C39M, 2003)	Cylinder	150 × 300 mm	7 Days
				14 Days
				21 Days
				28 Days
				56 Days
Splitting Tensile Strength	ASTM C496 (ASTM: C496/C496M – 17, 2011)	Cylinder	150 × 300 mm	28 Days
				56 Days
Flexural Strength	ASTM C78 (ASTM International, 2009)	Prism	100 × 100 × 500 mm	28 Days
				56 Days

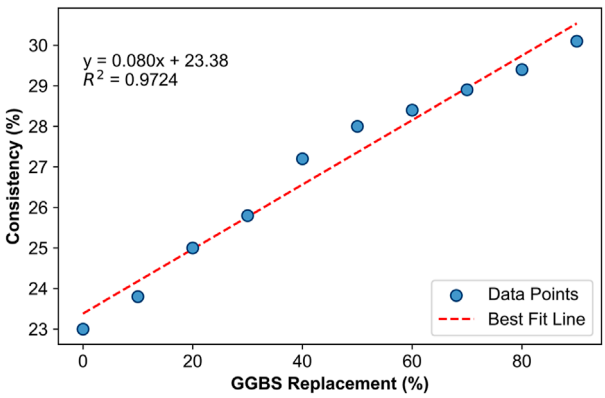

FIGURE 2
Water required for normal consistency of cement paste partially replaced with GGBS.

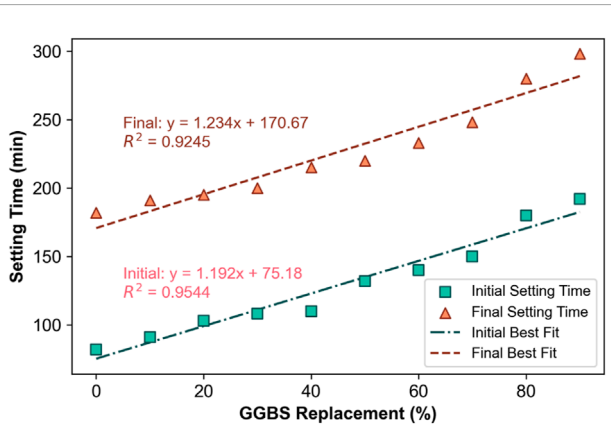

FIGURE 3
Initial and final setting time of cement paste partially replaced with GGBS.

between GGBS replacement level and the corresponding increases in setting times.

While a linear regression was applied here to describe the trend between GGBS replacement level and setting time, it is recognized that this approach is empirical in nature. For a more mechanistic understanding of the setting process, models such as the Avrami hydration kinetics equation could be applied in future studies to better capture the nucleation and growth behavior of hydration products in cement-GGBS systems (Sun et al., 2022).

4.2 Rheological properties of fresh concrete

4.2.1 Yield stress

Figures 4a–c illustrate the variation in yield stress for pumpable concrete across different GGBS replacement levels in all mix series. All mixes followed a general trend of increasing yield stress with time, an expected phenomenon reflecting ongoing hydration and structural build-up in the fresh cementitious system (Arularasi et al., 2021). During the early stages (first 30 min), the yield stress was comparatively low, promoting ease of flow and pumpability. As hydration products accumulated, intra-particle bonding became more pronounced, which raised the yield stress noticeably beyond the 30-minute mark.

In Mix Series A, which contains a higher cement-to-aggregate ratio, the larger paste volume contributed to a milder early increase in yield stress, indicating the mix retained sufficient fluidity to support pumping operations during the initial period. In contrast, the leaner mixes (Series B and Series C) had less paste available to lubricate the aggregates, thus displaying steeper increases in yield stress after the 30-min mark. These variations highlight how both paste content and mix proportions can influence the kinetics of structural build-up, highlighting the need to balance early workability with the desired rate of stiffening.

Figure 4d further illustrates the effect of increasing levels of GGBS on the yield stress for all mixes. In general, partial

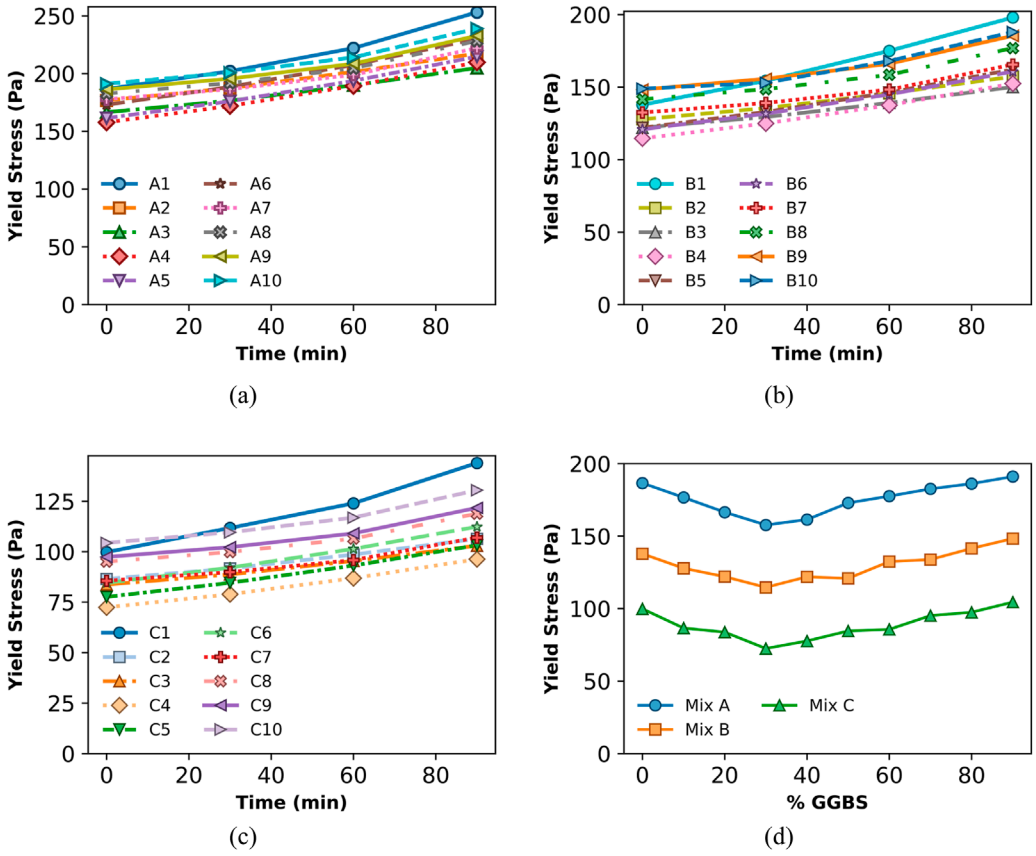

FIGURE 4
Evolution of Yield Stress of **(a)** Mix Series A, **(b)** Mix Series B, and **(c)** Mix Series C vs. time, and **(d)** Effect of GGBS Replacement on Yield Stress of All Mix Series.

replacements of cement with GGBS (e.g., 20%–40%) consistently lowered the initial yield stress, fostering enhanced workability and more extended pumpability windows. This improvement is primarily linked to GGBS particles refining the paste matrix, reducing internal friction, and prolonging the induction period of hydration, particularly in the early minutes after mixing.

These observations align well with the findings of Park et al. (2005), who studied the rheological behavior of cementitious systems incorporating GGBS using a cylindrical spindle rheometer. In their study, cement was partially replaced with GGBS at various levels. The results revealed that replacing cement with GGBS in the range of 15%–45% led to a noticeable reduction in yield stress, indicating improved flowability and workability of the concrete mixtures.

However, as the GGBS content increases beyond 50%, a more pronounced rise in yield stress is observed after the initial low values. This behavior results from the diminished OPC content, which reduces the availability of tricalcium silicate (C_3S), the main compound responsible for initiating early hydration. As a consequence, the dormant phase concludes more abruptly, and the activation of GGBS becomes the dominant source of hydration. Although this delayed activation initially promotes fluidity, it also leads to a steeper post-induction structuration due to the build-up of hydration products. The sudden stiffening effect, coupled with reduced OPC, can present challenges in pumping applications where extended flowability is needed. Therefore, while moderate GGBS levels optimize initial yield stress and enhance early workability, excessive replacement requires careful mix design control to avoid premature loss of flow during placement.

Past literature reports a similar trend in yield stress with increasing replacement of cement by GGBS. Several studies indicate that replacing cement with GGBS in the range of 15%–30% results in the lowest (i.e., optimum) yield stress, enhancing workability (Adjoudj et al., 2014; Amran et al., 2021). However, beyond this level, further increases in GGBS content tend to increase the yield stress, likely due to changes in particle packing and reduced early reactivity at high replacement levels (Montes et al., 2012).

Furthermore, at higher GGBS levels, the reduced calcium silicate content shifts the hydration mechanism toward aluminate-dominant reactions, particularly involving phases such as C_4AF and the alumina-rich components of GGBS. These aluminates can rapidly react with available sulfates, leading to early ettringite formation and localized flocculation, which contributes to the sudden yield stress increase observed after the dormant phase (Nedunuri and Muhammad, 2024). Additionally, chemical shrinkage from hydration reactions may enhance particle crowding in the paste, particularly under reduced OPC content, triggering early-age structuration and stiffening. These

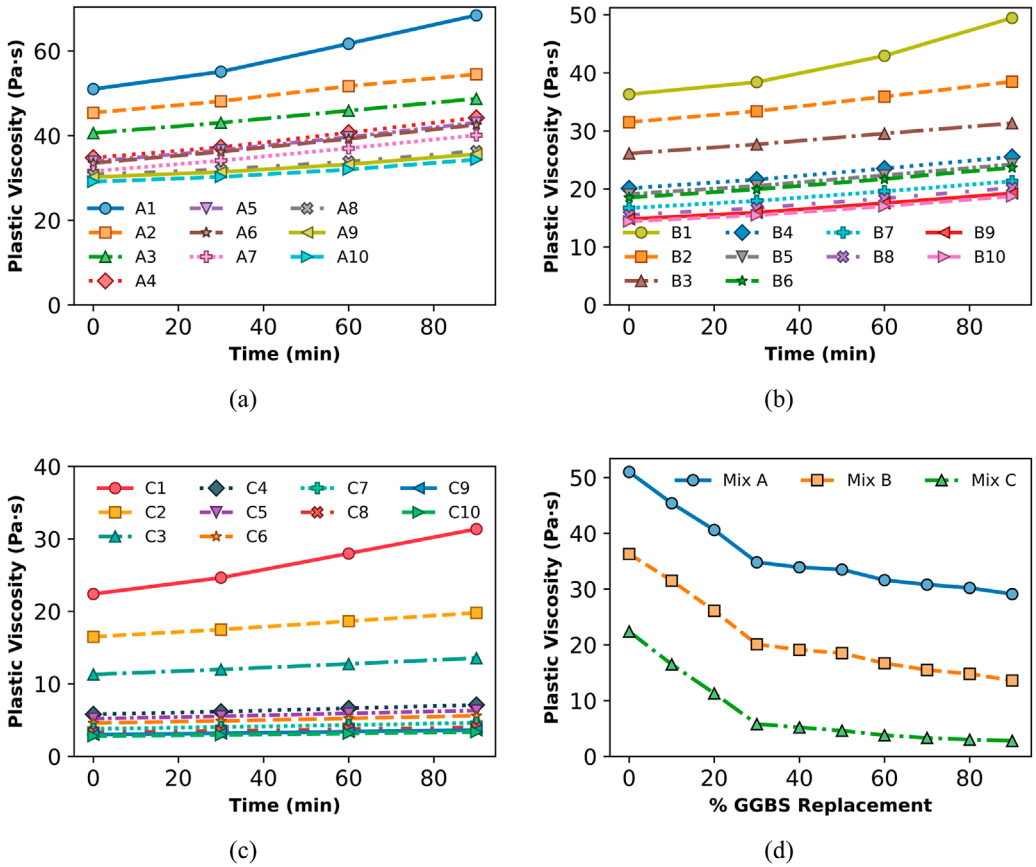

FIGURE 5
Evolution of Plastic Viscosity of **(a)** Mix Series A, **(b)** Mix Series B, and **(c)** Mix Series C vs. time, and **(d)** Effect of GGBS Replacement on Plastic Viscosity of All Mix Series at 0 min (freshly mixed state).

microstructural phenomena likely play a complementary role in the sharp rise in yield stress seen at GGBS levels exceeding 50%, and reinforce the importance of mix control when targeting extended pumpability.

4.2.2 Plastic viscosity

The plastic viscosity of all mix series was monitored over time to assess its evolution during the fresh state. Figures 5a–c illustrate the trends observed for each mix series. The results indicate that plastic viscosity generally increased with time, which can be attributed to the ongoing hydration of cementitious materials and the flocculation of particles in the fresh concrete. This phenomenon aligns with previous studies, which report that the time-dependent increase in plastic viscosity is primarily due to the progressive formation of hydration products and the reduction in free water available for lubrication (Ferraris, 2001; Roussel et al., 2010).

For Mix Series A, the plastic viscosity exhibited a steady increase over time, reflecting the gradual structuration of the cement paste. Similarly, Mix Series B showed a comparable trend, albeit with slightly higher initial plastic viscosity due to differences in mix design parameters. Interestingly, Mix Series C demonstrated a more pronounced increase in plastic viscosity over time, suggesting that specific mix proportions or admixture effects could be influencing the structuration rate.

The observed increase in plastic viscosity over time is a critical consideration in pumpability, as excessive stiffening of the mix during pumping could lead to blockages in pipelines. This highlights the importance of optimizing mix proportions and incorporating appropriate admixtures to regulate viscosity development.

The impact of GGBS replacement on plastic viscosity was analyzed for all mix series, as illustrated in Figure 5d. The values plotted in Figure 5d correspond to measurements taken at 0 min, i.e., immediately after mixing. The results indicate that increasing GGBS content generally led to a reduction in plastic viscosity. This decrease is primarily due to the finer particles and smooth surface texture of GGBS, which promote better particle packing and improve the dispersion of cementitious components. Consequently, the mix exhibits lower internal friction, resulting in reduced plastic viscosity.

Notably, the effect of GGBS replacement varied among the different mix series. In Mix Series A, incorporating GGBS resulted in a noticeable decline in plastic viscosity, particularly at higher replacement levels. The dilution effect and latent hydraulic activity of GGBS contribute to a less viscous paste. In Mix Series B, a similar trend was observed, albeit with a slightly less pronounced reduction in viscosity. This could be attributed to variations in mix proportions and water-to-binder ratios, which influence the overall rheological response.

Mix Series C exhibited a consistent reduction in plastic viscosity across all levels of GGBS replacement, reinforcing the idea that GGBS contributes positively to reducing the internal resistance to flow in fresh concrete. These findings align with previous studies, which highlight that GGBS reduces the overall viscosity of cement paste due to its lower water demand and enhanced dispersion characteristics (Vikan and Justnes, 2007).

While GGBS generally reduces plastic viscosity due to its spherical shape, high fineness, and lower water demand, this trend begins to plateau beyond 50% replacement. At such high levels, the dilution of OPC reduces the C-S-H framework formation in early hydration but increases alumina-based reactions, which can promote particle agglomeration and reduced fluid dispersion. Additionally, as superplasticizers are less effective in highly aluminate-rich environments, the dispersion efficiency may drop, leading to slight increases or stagnation in viscosity reduction. These effects, combined with increased paste volume and particle packing density, help explain the more complex plastic viscosity behavior observed at high GGBS levels.

The observed reduction in plastic viscosity with increasing GGBS content is consistent with the past studies (Grzeszczyk and Janowska-Renkas, 2012). For example, Park et al. (2005) explored the rheological behavior of cementitious systems containing mineral admixtures, including GGBS. They reported that partial replacement of cement with GGBS led to a notable decrease in plastic viscosity. This effect was attributed to the smoother particle morphology and lower early-age reactivity of GGBS, which helped reduce interparticle friction and enhance the dispersion of solid particles within the mix.

4.3 Mechanical properties

4.3.1 Compressive strength

Compressive strength is a key parameter for assessing the structural performance and load-bearing capacity of concrete. It directly governs the load-bearing capacity, durability, and serviceability of concrete in construction applications. In pumpable concrete, compressive strength is significantly influenced by concrete composition, water-to-cement ratio, admixture content, and the fractional substitution of cement with GGBS.

The incorporation of GGBS as an SCM enhances long-term strength development, but at the cost of lower early-age strength due to its slower pozzolanic reaction (Monteiro, 2006). This research investigated the compressive strength performance of 30 pumpable concrete mixes, comprising three series (A, B, and C), each with GGBS content varying from 0% to 90%. The compressive strength was measured at 7, 14, 21, 28, and 56 days, ensuring a comprehensive understanding of strength development trends. The experimental values are presented in Figure 6, illustrating the result of curing (age) and GGBS content on compressive-strength performance.

At early ages (7–21 days), the results indicate a decrease in compressive strength as the GGBS content increases. This is primarily due to the slower initial hydration reaction of GGBS compared to OPC, leading to delayed strength gain (Monteiro, 2006). The trends show that low GGBS content (0%–20%) exhibits higher early-age strength, as OPC dominates the hydration process. With moderate GGBS content (30%–50%), early-age strength is slightly reduced but remains sufficient for practical applications. However, a high GGBS content (exceeding 50%) leads to noticeably reduced early-age strength, primarily due to the slower pozzolanic activity of GGBS. These findings align with studies by Oh et al. (2024) and Li et al. (2014), which reported delayed early-age strength development in GGBS-based concrete.

Notably, Series A (1:1:2), with richer cement content, shows comparatively higher early-age strengths across all GGBS replacement levels, while Series C (1:3:6), being the leanest mix, consistently yields lower strengths at these ages. Series B (1:2:4) lies between these two extremes. Despite these differences, the general trend of reduced early strength with higher GGBS replacement remains consistent across all three series.

Regarding later-age strength gain (28 and 56 days), the pozzolanic activity of GGBS accelerates, leading to continued strength development beyond 28 days. Most mixes containing GGBS catch up or surpass the control mix by 56 days. The enhancement in strength is primarily due to the increased formation of calcium silicate hydrate (C-S-H) gel, which strengthens the concrete's microstructure. Furthermore, improved matrix densification and lower porosity contribute to higher compressive strength at later curing stages, as supported by microstructural evidence in previous studies (He and Lu, 2024a; He et al., 2024). It is important to note that this explanation is based on indirect mechanical evidence and literature precedent. No direct microstructural validation (e.g., SEM, MIP) was performed in this study. Therefore, the interpretation of C-S-H densification remains speculative and should be confirmed through future microstructural analyses.

The results show that, at 28 days, the maximum compressive strength is typically achieved with a 40% GGBS replacement level across all three mix series (A, B, and C). By 56 days, mixes within the 30%-50% GGBS range show the highest strengths, often exceeding the strength of the control mix (0% GGBS). For instance, in Series A, the peak 56-day strength (49.5 MPa) is achieved at 40% GGBS content. Beyond 50% GGBS, strength continues to increase with curing time but remains lower compared to the 30%–50% range. These findings align with previous research (Chen et al., 2024), where GGBS improved long-term strength but required extended curing durations to match or exceed OPC concrete strength.

An interesting observation is that even with high GGBS content (e.g., 90%), later-age strengths can still reach structurally viable strength under carefully managed laboratory conditions. For Series A, 90% GGBS and 10% OPC can yield a 56-day compressive strength of about 37.5 MPa, provided that the mix design includes a suitably low water-to-binder ratio, adequate superplasticizer dosage, and proper curing. Although early-age strength (7–21 days) is significantly reduced at these high replacement levels, the slower pozzolanic reaction of GGBS can still lead to substantial long-term strength when given sufficient curing time and favorable conditions (Monteiro, 2006). Nevertheless, for practical purposes, such high-volume GGBS mixes may not be ideal where early strength is critical.

The results confirm that low GGBS content (0%–20%) maintains high early-age strength but does not offer the most significant long-term benefits. Conversely, moderate GGBS content (30%–50%) achieves the best balance between early-age and later-age strength, making it ideal for structural applications requiring good workability, pumpability, and enhanced durability. High GGBS

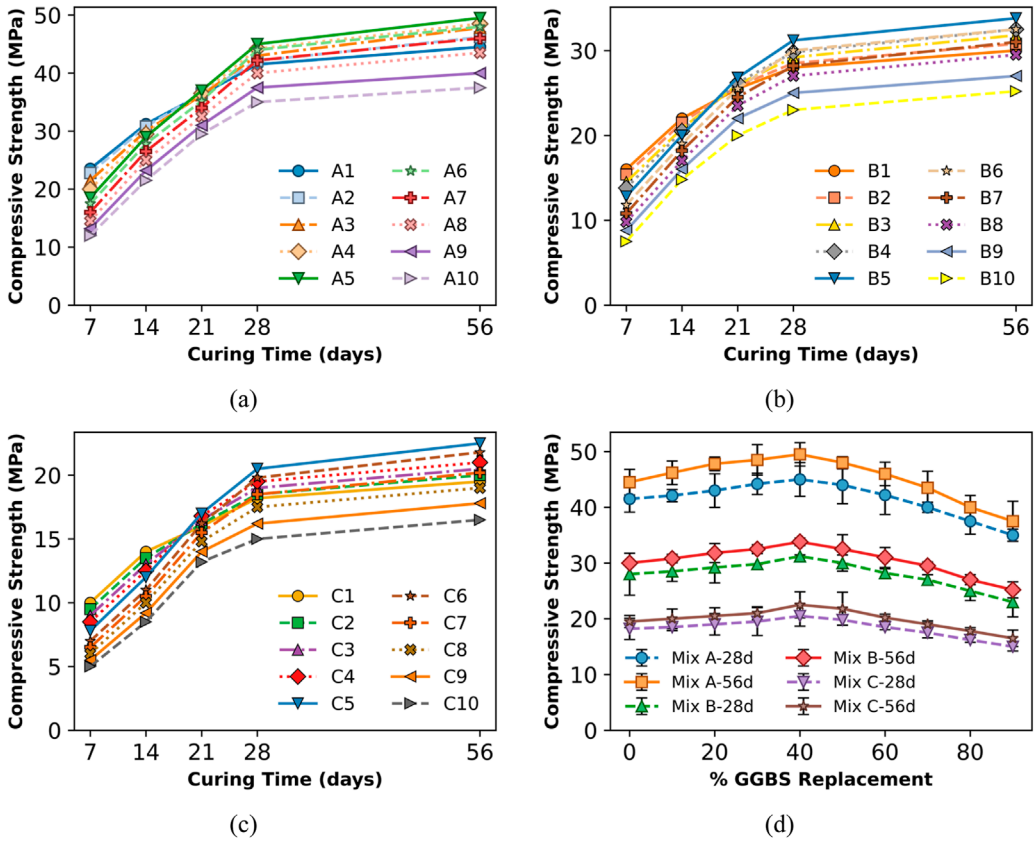

FIGURE 6
Compressive strength of **(a)** mix series A, **(b)** mix series b, and **(c)** mix series C at 7, 14, 21, 28, and 56 days, and **(d)** effect of GGBS replacement on compressive strength at 28 and 56 Days.

content (>50%) excessively delays strength gain and reduces the 28-day strength, although continued curing can still improve the final strength somewhat. As illustrated in Figure 6d, the maximum compressive strength at 28 and 56 days was specifically observed at 40% GGBS replacement. Although mixes with 30% and 50% GGBS also showed considerable long-term gains, exceeding 50% GGBS generally resulted in lower 28-day strength due to the dilution of OPC and slower hydration reactions. These findings are consistent with previous studies suggesting that an optimal GGBS replacement range for concrete lies between 30% and 50% (Ganesh and Murthy, 2019).

While the observed strength enhancement at moderate GGBS levels is likely associated with increased C-S-H formation and matrix densification, this explanation remains interpretative. Since the present study does not include microstructural validation techniques (e.g., SEM or MIP), the proposed mechanisms are based on indirect evidence from mechanical trends. Future studies incorporating such analyses could more definitively verify these observations.

4.3.2 Splitting tensile strength

Cracking in hardened concrete initiates when the locally induced tensile stress exceeds the concrete's intrinsic tensile capacity. The Splitting Tensile Strength, obtained in compliance with ASTM C496 (ASTM: C496/C496M – 17, 2011), is therefore a direct indicator of the stress level at which first micro-cracks form under restraint loading. Likewise, the Flexural Strength or Modulus of Rupture (ASTM C78 (ASTM International, 2009)) governs crack initiation and propagation under bending; it is the parameter used in serviceability-limit calculations for pavements, slabs and beams. Mixtures that exhibit higher Splitting Tensile and Flexural Strength delay crack initiation, reduce crack spacing, and limit crack widths, thereby restricting the ingress of aggressive agents such as chlorides, sulfates and CO_2. Numerous durability models (e.g., fib Model Code 2010 (Taerwe and Matthys, 2013), ACI 546) embed these parameters when predicting service-life or allowable crack width.

Since concrete is inherently poor in tension, its splitting tensile strength is significantly influenced by the mix proportions, aggregate interlocking, paste cohesion, and hydration reactions (Neville, 2011). The effect of GGBS replacement, w/c ratio, and superplasticizer dosage on splitting tensile strength was investigated at 28 and 56 days, with results illustrated in Figure 7.

The results confirm that splitting tensile strength increases with curing age, aligning with the findings of Güneyisi et al. (2013), who observed a similar gain in tensile resistance due to continued hydration and pozzolanic reactions. At 28 days, mixes with low GGBS content (0%–30%) exhibit higher splitting tensile strength because of the early strength contribution of OPC hydration (Ramzi and Hajiloo, 2023).

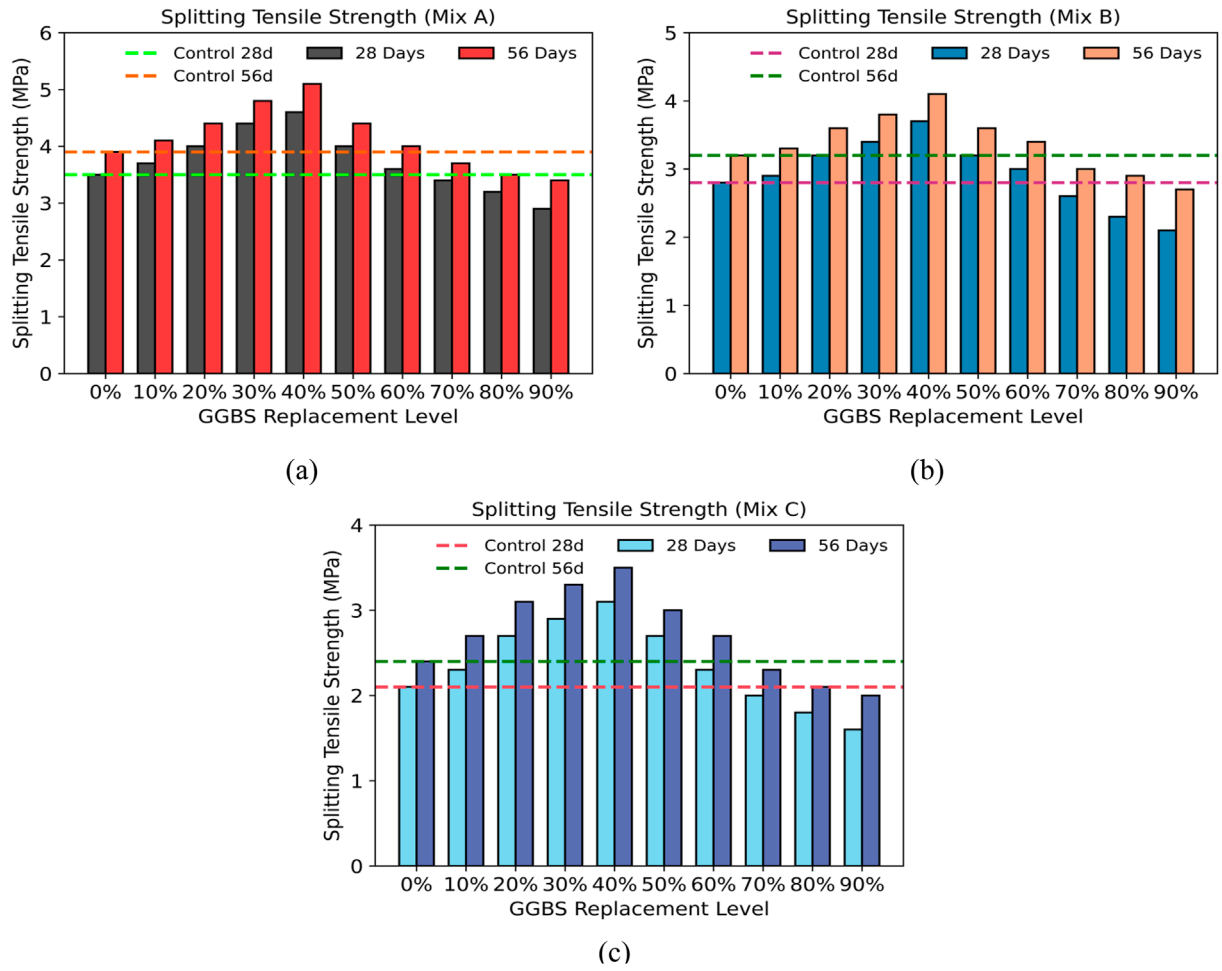

FIGURE 7
Splitting Tensile Strength of **(a)** Mix Series A, **(b)** Mix Series B, and **(c)** Mix series C at 28 and 56 Days.

The highest splitting tensile strength at 28 days was observed at 40% GGBS replacement, with Mix A5 achieving 4.6 MPa, Mix B5 reaching 3.7 MPa, and Mix C5 attaining 3.1 MPa. At 56 days, an increase in tensile strength is observed across all mixes, with the maximum tensile strength still recorded at 40% GGBS replacement. Mix A5 achieves 5.1 MPa, Mix B5 reaches 4.1 MPa, and Mix C5 records 3.5 MPa, confirming that 40% GGBS replacement provides the optimal balance for splitting tensile strength improvement. These results align with the pozzolanic reaction that enhances the binding properties of the paste over time, as also observed by Venkitasamy et al. (Venkitasamy et al., 2024).

Beyond 40% GGBS replacement, a decreasing trend is observed, suggesting that excessive GGBS incorporation leads to higher paste viscosity, poor aggregate bonding, and delayed hydration effects, leading to tensile strength reduction (Siddique, 2014). Mixes with high GGBS content exhibited the lowest tensile strengths at both 28 and 56 days, with Mix A10, B10, and C10 showing 2.9 MPa, 2.1 MPa, and 1.6 MPa at 28 days, respectively, and further reductions at 56 days.

A direct correlation between compressive and splitting tensile strength is observed, consistent with past research. The optimal replacement range (30%–50% GGBS) ensures both compressive and tensile strength enhancement, making it ideal for structural applications requiring high durability. Excessive GGBS replacement (>50%) adversely affects early-age compressive and tensile strength, suggesting that beyond this limit, GGBS inclusion leads to excessive cohesiveness and lower aggregate-paste bonding (Sankar and Ramadoss, 2022).

As illustrated in Figure 7, horizontal reference lines indicate the control mix's 28-day and 56-day splitting tensile strengths, allowing a clear comparison of each GGBS-based mixture against the baseline. With respect to tensile strength, the results show that mixes incorporating 30%–50% GGBS either match or outperform the control mix, while higher replacement levels generally lead to a decline in performance, reinforcing 40% GGBS as the optimal replacement level.

Splitting tensile strength, unlike compressive strength, is more directly influenced by the formation and propagation of internal microcracks and the quality of the paste–aggregate bond. At moderate GGBS levels (30%–40%), enhanced matrix packing and reduced porosity support better crack resistance. However, at higher GGBS levels, the slower pozzolanic activation can weaken

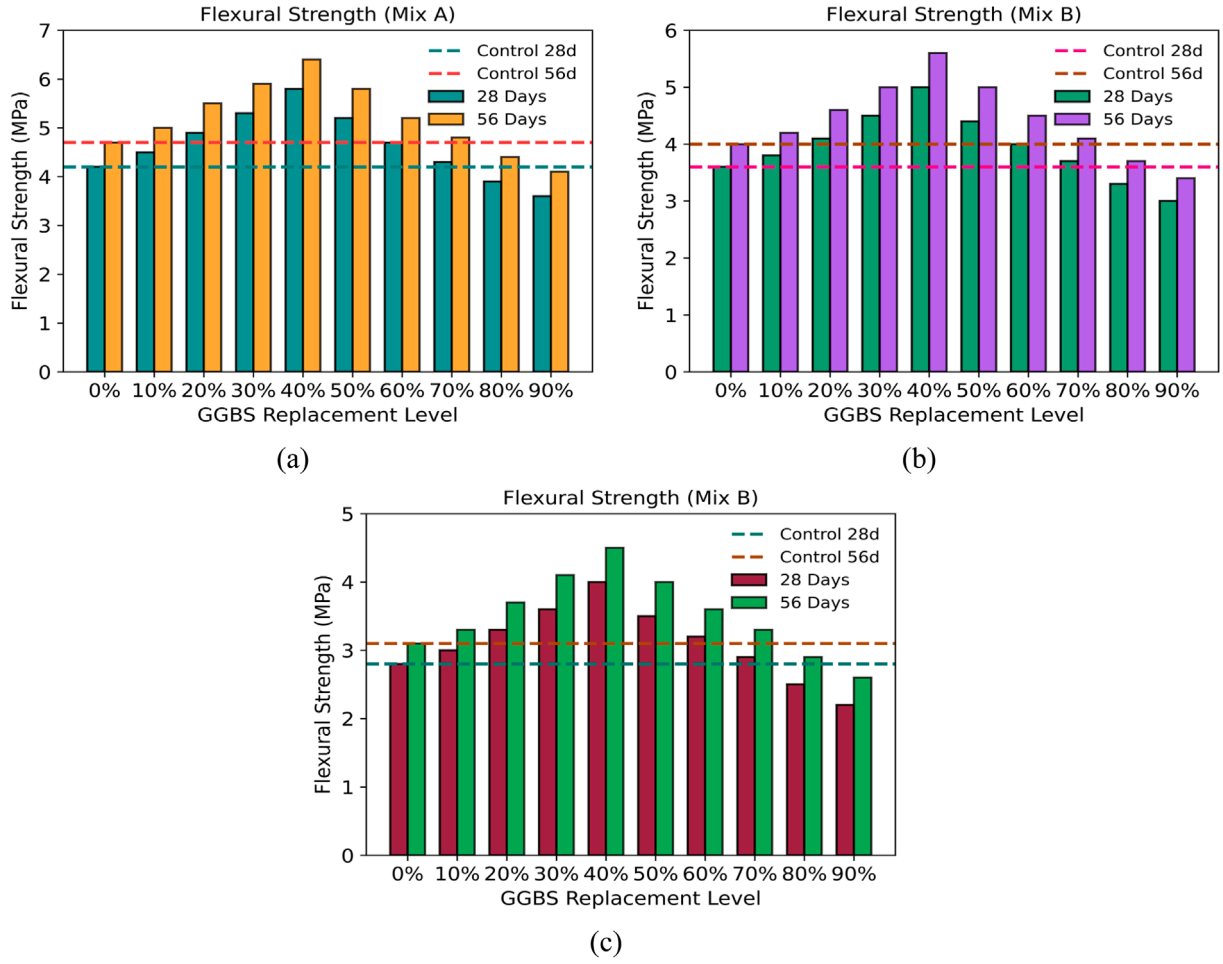

FIGURE 8
Flexural Strength of **(a)** Mix Series A, **(b)** Mix Series B, and **(c)** Mix series C at 28 and 56 Days.

early-age ITZ development, potentially leading to microstructural discontinuities that impair tensile resistance. These observations align with studies where tensile performance has been linked to early microcracking behavior and delayed matrix cohesion in GGBS-blended systems (He et al., 2024).

4.3.3 Flexural strength

Flexural strength is an essential mechanical property that evaluates the ability of concrete to resist bending stresses, particularly in beam and slab structures. The flexural performance of pumpable concrete is significantly influenced by the mix composition, w/c ratio, GGBS replacement level, and curing age. Partially replacing cement with GGBS modifies the hydration process, which in turn influences the flexural strength of concrete over time. The flexural strength results for all 30 mix designs were evaluated at 28 and 56 days. The age-dependent flexural strength development is presented in Figures 8a–c, which demonstrate the flexural strength variations for Mix A, Mix B, and Mix C, respectively. At 28 days, the results indicate a steady increase in flexural strength with increasing GGBS replacement up to 40%, beyond which a decline is observed. The maximum flexural strength at 28 days was recorded at 40% GGBS replacement, with Mix A5 achieving 5.8 MPa, Mix B5 reaching 5.0 MPa, and Mix C5 attaining 4.0 MPa. This trend aligns with previous studies (Dom et al., 2022) attributing the improvement at moderate GGBS levels to the pozzolanic activity of GGBS, which leads to the formation of secondary C-S-H gel, enhancing the matrix's load-bearing capacity.

At 56 days, most of the mixes demonstrated continued strength gain, indicating the prolonged hydration process facilitated by GGBS reactivity at later ages. Similar to compressive and splitting tensile strength trends, Mixes with 40% GGBS consistently achieved the highest flexural strength at 56 days. The extended curing period allowed for increased pozzolanic reactions, forming additional C-S-H gel, which improved the tensile load distribution capacity (Ayub et al., 2014). However, for mixes exceeding 50% GGBS replacement, the continued strength gain was relatively lower due to the lack of sufficient OPC content, which is essential for initiating early hydration and strength development.

The relationship between flexural strength and GGBS replacement at 28 and 56 days is illustrated in Figure 8d. The results indicate that low GGBS content (0%–20%) results in lower flexural strength due to the lack of supplementary pozzolanic reactions, which are essential for improving the concrete matrix's

tensile resistance. In contrast, moderate GGBS content (30%–50%) provides optimum flexural performance, enhancing load transfer capability and minimizing microcracking under bending stresses. This is attributed to the increased formation of C-S-H gel, which strengthens the bond between the aggregates and the cementitious matrix. However, at high GGBS content (>50%), a noticeable decline in flexural strength occurs, likely owing to the excessive dilution of OPC and increased porosity, which weakens the mix's ability to resist tensile stresses (Samad and Shah, 2017).

These findings align with past studies (Karri et al., 2015; Ahmad et al., 2022), which emphasize that an optimum range of 30%–50% GGBS replacement maximizes mechanical properties without compromising early-age strength. The results further confirm that while GGBS enhances long-term mechanical properties, excessive replacement reduces early-age strength and negatively impacts flexural behavior. Therefore, careful optimization of GGBS content is essential to achieve a balance between workability, strength, and long-term performance, ensuring structural integrity in high-performance applications.

A comparative analysis of Mix A, B, and C shows that Mix A exhibited the highest flexural strength, followed by Mix B and then Mix C. This can be attributed to the lower w/c ratio in Mix A, leading to a denser and more compact concrete matrix. Mix C, having the highest w/c ratio, exhibited the lowest flexural strength due to increased porosity and reduced cohesion between cementitious particles. These patterns align with the results observed in compressive and splitting tensile strength, highlighting the interconnected nature of concrete strength properties.

Flexural strength is particularly governed by how well tensile stresses are redistributed across the cross-section and how effectively cracks are bridged at the bottom fiber. In this context, the bond between coarse aggregates and paste plays a dominant role. Moderate GGBS content improves ITZ characteristics, resulting in higher energy absorption and delayed crack widening under flexural loading. However, at GGBS levels above 50%, reduced early hydration limits the formation of a dense bond network, which can initiate premature cracking and more brittle behavior—especially in leaner mixes like Series C. Prior microstructural research has linked such flexural failure modes to insufficient ITZ formation during early curing (He and Lu, 2024b).

In this study the mixes containing 30%–50% GGBS achieved the highest Splitting Tensile and Flexural Strength, which implies a lower risk of early micro-cracking and, consequently, enhanced long-term durability through improved resistance to deleterious ion penetration and freeze–thaw damage. These observations are consistent with the crack-resistance mechanisms reported by Neville (2011) and Venkitasamy et al. (2024) for tensile behaviour, and by Dom et al. (2022) for flexural performance, reinforcing the durability benefits of moderate GGBS replacement.

5 Conclusion

This study investigated the effects of GGBS as a partial replacement for OPC on the rheological and mechanical characteristics of pumpable concrete. From the experimental observations, the following conclusions are evident:

1. The consistency of cement paste increased with higher GGBS replacement levels, primarily due to the finer particle size and higher specific surface area of GGBS, which led to greater water retention.
2. Both the initial and final setting times of the cement paste showed a gradual increase as the GGBS content was raised. At 90% GGBS replacement, the initial setting time was extended to 192 min, while the final setting time reached 298 min. The delay in setting time is attributed to the lower availability of tricalcium silicate (C_3S) in GGBS, which slows down the early hydration process. While this delay can be beneficial for mass concrete applications, it may present challenges in rapid construction projects requiring early strength development.
3. The incorporation of GGBS significantly improved the flowability and pumpability of fresh concrete by reducing both yield stress and plastic viscosity, with an optimal replacement range of 30%–50%, ensuring workability and stability without segregation. Over time, yield stress and plastic viscosity increased due to progressive hydration and structuration of the cement paste, affecting the pumpability of concrete. The use of 30%–50% GGBS effectively delayed early stiffening, maintaining a longer pumpability window. However, at higher GGBS levels (>50%), excessive viscosity reduction increased the risk of bleeding and segregation, while yield stress showed a sharper rise after the dormant phase, requiring careful mix optimization to prevent sudden stiffening during extended pumping.
4. Early-age (7–21 days) compressive strength decreased with increasing GGBS content due to its slower pozzolanic reaction. At 28 days, concrete with 30%–50% GGBS replacement achieved compressive strengths comparable to or higher than the control mix. By 56 days, GGBS-incorporated mixes exhibited superior strength performance, with 40% GGBS replacement yielding the highest compressive strength.
5. Splitting tensile and flexural strength results followed trends similar to compressive strength, with peak values observed at 40% GGBS replacement. At lower GGBS levels (10%–20%), minimal improvement in tensile strength was observed compared to the control mix. Higher replacement levels (>50%) led to a decline in tensile and flexural strength due to reduced early-age cement hydration and matrix cohesion.

While this study identifies 30%–40% GGBS as the optimal replacement range for balancing strength and workability, this conclusion is specific to the materials, water-to-binder ratio, superplasticizer type, mix proportions, and curing conditions adopted in our experiments. The optimal level of GGBS replacement may vary in other contexts, especially under different ambient temperatures, binder chemistries, admixture systems, or curing regimes. Therefore, while these findings provide useful design guidance, they should be applied with caution beyond the boundaries of the present study.

5.1 Limitations and future works

Although this study provides detailed insights into the mechanical and rheological performance of pumpable concrete with

GGBS, a key limitation is the absence of microstructural analysis such as SEM or MIP to directly validate the proposed mechanisms of C-S-H densification and pore refinement. Future research should incorporate such techniques to provide more definitive evidence supporting the strength development and durability trends observed in this work.

Data availability statement

The original contributions presented in the study are included in the article/supplementary material, further inquiries can be directed to the corresponding authors.

Author contributions

HA: Formal Analysis, Methodology, Writing – review and editing, Investigation, Conceptualization, Writing – original draft. TP: Writing – review and editing, Funding acquisition, Supervision, Validation. MA: Formal Analysis, Investigation, Data curation, Writing – original draft, Methodology. MK: Software, Resources, Writing – review and editing, Methodology. MR: Software, Formal Analysis, Writing – review and editing, Conceptualization, Data curation.

Funding

The author(s) declare that financial support was received for the research and/or publication of this article. This research was supported by the National Natural Science Foundation of China under Grant Nos. 51278372 and 51878489.

Conflict of interest

The authors declare that the research was conducted in the absence of any commercial or financial relationships that could be construed as a potential conflict of interest.

Generative AI statement

The author(s) declare that Generative AI was used in the creation of this manuscript. Artificial intelligence tools, specifically OpenAI's ChatGPT 4.0, were used to improve the grammar, clarity, and structure of the manuscript. The authors confirm that all core ideas, data analysis, experimental design, interpretation of results, and conclusions were developed by the authors. The use of AI was limited to editorial assistance and did not influence the scientific content or integrity of the work.

Publisher's note

All claims expressed in this article are solely those of the authors and do not necessarily represent those of their affiliated organizations, or those of the publisher, the editors and the reviewers. Any product that may be evaluated in this article, or claim that may be made by its manufacturer, is not guaranteed or endorsed by the publisher.

References

A. ASTM C150 (2017). Astm C150/C150M-22. *Stand. Specif. Portl. Cem.*, 1–8. doi:10.1520/C0150_C0150M-17

Adjoudj, M., Ezziane, K., Ngo, T.-T., and Kaci, A. (2014). Evaluation of rheological parameters of mortar containing various amounts of mineral addition with polycarboxylate superplasticizer. *Constr. Build. Mater.* 70, 549–559. doi:10.1016/j.conbuildmat.2014.07.111

Ahmad, J., Kontoleon, K. J., Majdi, A., Naqash, M. T., Deifalla, A. F., Ben Kahla, N., et al. (2022). A comprehensive review on the ground granulated blast furnace slag (GGBS) in concrete production. *Sustainability* 14 (14), 8783. doi:10.3390/su14148783

Ajmal, M. M., Qazi, A. U., Ahmed, A., Mughal, U. A., Abbas, S., Kazmi, S. M. S., et al. (2023). Structural performance of energy efficient geopolymer concrete confined masonry: an approach towards decarbonization. *Energies* 16 (8), 3579. doi:10.3390/en16083579

Akhlaq, H., Butt, F., Alwetaishi, M., Riaz, M., Benjeddou, O., and Hussein, E. E. (2022). Structural identification of a 90 m high minaret of a landmark structure under ambient vibrations. *Buildings* 12 (2), 252. doi:10.3390/buildings12020252

Akhlaq, H., Peng, T., Jitteh, K., and Khan, M. S. (2025b). Machine learning models for predicting seismic response of a novel two-stage friction pendulum isolated bridge structure. *IEEE Access* 13, 105165–105182. doi:10.1109/access.2025.3580065

Akhlaq, H., Peng, T., Yan, B., and Khan, M. S. (2025a). Development and verification of a new OpenSees element model for a two-stage friction pendulum bearing. *Sci. Rep.* 15 (1), 22763. doi:10.1038/s41598-025-02928-6

Alkuhly, M. (2021). *Studies of self-compacting concrete containing GGBS*. Cardiff, Wales: Cardiff University.

Amran, M., Murali, G., Khalid, N. H. A., Fediuk, R., Ozbakkaloglu, T., Lee, Y. H., et al. (2021). Slag uses in making an ecofriendly and sustainable concrete: a review. *Constr. Build. Mater.* 272, 121942. doi:10.1016/j.conbuildmat.2020.121942

Arularasi, V., Thamilselvi, P., Avudaiappan, S., Saavedra Flores, E. I., Amran, M., Fediuk, R., et al. (2021). Rheological behavior and strength characteristics of cement paste and mortar with fly ash and GGBS admixtures. *Sustainability* 13 (17), 9600. doi:10.3390/su13179600

Astm (2004). Standard test method for normal consistency of hydraulic cement, C 187 – 04. *Astm* i (C), 1–3. doi:10.1520/C0187-10.2

ASTM (2014). C143/C143M – 12, "standard test method for slump of hydraulic cement concrete,". *ASTM Int.*, 1–4.

ASTM C127 (2001). Standard test method for specific gravity and water absorption of coarse aggregate. *Am. Soc. Test. Mater.* 04, 1–6.

ASTM C143/C143M (2015). Standard test method for slump of hydraulic-cement concrete. *Astm* C143 (1), 1–4. doi:10.1520/C0143

ASTMC191-08 (2009). Standard test methods for time of setting of hydraulic cement by Vicat needle. *ASTM Int.* 04 (C), 1–8. Available online at: www.astm.org.

ASTM-C311-11 (2019). Standard test methods for sampling and testing coal ash or natural pozzolans for use in concrete. *Annu. B. ASTM Stand. Am. Soc. Test. Mater.* 4 (8), 11. doi:10.1520/C0311-11

ASTM: C39/C39M (2003). Standard test method for compressive strength of cylindrical concrete specimens 1. *ASTM Stand. B.* i (March), 1–5. doi:10.1520/C0039_C0039M-03

ASTM C494 (2005). *Astm C494/C949M-19: standard specification for chemical admixtures for concrete*, C494. January: Astm, 1–10.

ASTM: C496/C496M – 17 (2011). *Standard test method for splitting tensile strength of cylindrical concrete specimens ASTM C-496*. PA, United States: ASTM Int., 1–5.

ASTM C989 (2004). *Standard specification for ground granulated blast-furnace slag for use in concrete and mortars*. PA, United States: ASTM Int., 1–5.

ASTM International, (2025). *AASTM C1749-25: Standard guide for measurement of the rheological properties of hydraulic cementitious paste using a rotational rheometer*. West Conshohocken, PA: ASTM International

ASTM International (2019). ASTM C136/C136M standard test method for sieve analysis of fine and coarse aggregates. *ASTM Stand*, 3–7.

ASTM International (2009). *ASTM C78-09: Standard test method for flexural strength of concrete (using simple beam with third-point loading)*. West Conshohocken, PA: ASTM International. doi:10.1520/C0078_C0078M-16

Ayub, T., Khan, S. U., and Memon, F. A. (2014). Mechanical characteristics of hardened concrete with different mineral admixtures: a review. *Sci. World J.* 2014 (1), 1–15. doi:10.1155/2014/875082

Banfill, P. F. G. (1990). *Rheology of fresh cement and concrete: proceedings of an international conference, liverpool, 1990*. London, United Kingdom: CRC Press.

Basit, A., Abbas, S., Ajmal, M. M., Mughal, U. A., Kazmi, S. M. S., and Munir, M. J. (2024). Joint behavior of full-scale precast concrete pipe infrastructure: experimental and numerical analysis. *Infrastructures* 9 (4), 69. doi:10.3390/infrastructures9040069

Binns, T. (2003). "Pumped concrete," in *Advanced concrete technology* (Elsevier), 1–33.

Chen, W., Wu, M., and Liang, Y. (2024). Effect of SF and GGBS on pore structure and transport properties of concrete. *Mater. (Basel)* 17 (6), 1365. doi:10.3390/ma17061365

Documents, R., and Information, O. (2005). *Standard practice for ultrasonic*, 1–6.

Dom, A. A. M., Jamaluddin, N., Hamid, N. A. A., and Hoon, C. S. (2022). A review: GGBS as a cement replacement in concrete. *IOP Conf. Ser. Earth Environ. Sci.* 1022 (1), 12044. doi:10.1088/1755-1315/1022/1/012044

Ferraris, C. F., Brower, L. E., Banfill, P., Beaupré, D., Chapdelaine, de Larrard, F., et al. (2001). *Comparison of concrete rheometers: international test at LCPC (Nantes, France) in October, 2000*. Gaithersburg, MD: US Department of Commerce, National Institute of Standards and Technology.

Feys, D., De Schutter, G., Khayat, K. H., and Verhoeven, R. (2016). Changes in rheology of self-consolidating concrete induced by pumping. *Mater. Struct.* 49, 4657–4677. doi:10.1617/s11527-016-0815-7

Feys, D., Verhoeven, R., and De Schutter, G. (2007). Evaluation of time independent rheological models applicable to fresh self-compacting concrete. *Appl. Rheol.* 17 (5), 56244–10. doi:10.1515/arh-2007-0018

Ganesh, P., and Murthy, A. R. (2019). Tensile behaviour and durability aspects of sustainable ultra-high performance concrete incorporated with GGBS as cementitious material. *Constr. Build. Mater.* 197, 667–680. doi:10.1016/j.conbuildmat.2018.11.240

Gee, K. H. (1979). "The potential for slag in blended cements," in *Proceedings, 14th international cement seminar, rock products*, 53–55.

Grzeszczyk, S., and Janowska-Renkas, E. (2012). The influence of small particle on the fluidity of blast furnace slag cement paste containing superplasticizers. *Constr. Build. Mater.* 26 (1), 411–415. doi:10.1016/j.conbuildmat.2011.06.040

Güneyisi, E., Gesoğlu, M., and Algin, Z. (2013). *Performance of self-compacting concrete (SCC) with high-volume supplementary cementitious materials (SCMs)*. Eco-Efficient Concr., 198–217.

He, R., and Lu, N. (2024a). Air void system and freezing-thawing resistance of concrete composite with the incorporation of thermo-expansive polymeric microspheres. *Constr. Build. Mater.* 419, 135535. doi:10.1016/j.conbuildmat.2024.135535

He, R., and Lu, N. (2024b). Hydration, fresh, mechanical, and freeze-thaw properties of cement mortar incorporated with polymeric microspheres. *Adv. Compos. Hybrid. Mater.* 7 (3), 92. doi:10.1007/s42114-024-00899-2

He, R., Nantung, T., and Luna) Lu, N. (2024). Unraveling microstructural evolution in air-entrained mortar and paste: insights from MIP and micro-CT tomography amid cyclic freezing-thawing damage. *J. Build. Eng.* 94, 109922. doi:10.1016/j.jobe.2024.109922

International, A., ASTM C-191, (2008). Time of setting of hydraulic cement by Vicat needle. *Annu. B. ASTM Stand.* 191-04 (C), 1–10.

Kaplan, D., De Larrard, F., and Sedran, T. (2005). Avoidance of blockages in concrete pumping process. *ACI Mater. J.* 102 (3), 183.

Karri, S. K., Rao, G. V. R., and Raju, P. M. (2015). Strength and durability studies on GGBS concrete. *SSRG Int. J. Civ. Eng.* 2 (10), 34–41. doi:10.14445/23488352/IJCE-V2I10P106

Khan, M. S., Peng, T., Akhlaq, H., and Khan, M. A. (2025). Comparative analysis of automated machine learning for hyperparameter optimization and explainable artificial intelligence models. *IEEE Access* 13, 84966–84991. doi:10.1109/access.2025.3566427

Lawrence, A. M., Tia, M., Ferraro, C. C., and Bergin, M. (2012). Effect of early age strength on cracking in mass concrete containing different supplementary cementitious materials: experimental and finite-element investigation. *J. Mater. Civ. Eng.* 24 (4), 362–372. doi:10.1061/(asce)mt.1943-5533.0000389

Li, Q., Yuan, G., Xu, Z., and Dou, T. (2014). Effect of elevated temperature on the mechanical properties of high-volume GGBS concrete. *Mag. Concr. Res.* 66 (24), 1277–1285. doi:10.1680/macr.14.00142

Liew, J. J., Cheah, C. B., Khaw, K. L. P., Siddique, R., and Tangchirapat, W. (2024). Blended cement and mortar with various low-calcium ground coal bottom ash content: engineering characteristics, embodied carbon and cost analysis. *Constr. Build. Mater.* 425, 135987. doi:10.1016/j.conbuildmat.2024.135987

Malhotra, V. M. (2000). Role of supplementary cementing materials in reducing greenhouse gas emissions. *Concr. Technol. a Sustain. Dev. 21st century* 5, 6.

Mark, O. G., Ede, A. N., Olofinnade, O., Bamigboye, G., Okeke, C., Oyebisi, S. O., et al. (2019). Influence of some selected supplementary cementitious materials on workability and compressive strength of concrete–A Review. *IOP Conf. Ser. Mater. Sci. Eng.* 640 (1), 012071. doi:10.1088/1757-899x/640/1/012071

Monteiro, P. (2006). *Concrete: microstructure, properties, and materials*. McGraw-Hill Publishing.

Montes, C., Zang, D., and Allouche, E. N. (2012). Rheological behavior of fly ash-based geopolymers with the addition of superplasticizers. *J. Sustain. Cem. Mater.* 1 (4), 179–185. doi:10.1080/21650373.2012.754568

Nadir, H. M., and Ahmed, A. (2022). The mechanisms of sulphate attack in concrete–a review. *Mod. Approaches Mater. Sci.* 5 (2), 658–670. doi:10.32474/MAMS.2022.05.000206

Nedunuri, A. S. S. S., and Muhammad, S. (2024). Development and field validation of pumpable alkali-activated ground granulated blast furnace slag binder-based concrete using sodium gluconate as a retarder. *J. Build. Eng.* 98, 111295. doi:10.1016/j.jobe.2024.111295

Neville, A. M. (2011). *Properties of concrete, pearson education limited*. Edinburgh Gate: Harlow Engl, 58–661.

Nguyen, Q. D., and V Boger, D. (1992). Measuring the flow properties of yield stress fluids. *Annu. Rev. Fluid Mech.* 24 (1), 47–88. doi:10.1146/annurev.fl.24.010192.000403

Oh, S., Kim, J., Song, C., and Choi, S. (2024). Effects of fineness and substitution rate of GGBFS on material characteristics of GGBFS-blended cement mortars: hydration, non-evaporable water, pore structure, mechanical properties, self-desiccation, and autogenous shrinkage. *J. Build. Eng.* 92, 109741. doi:10.1016/j.jobe.2024.109741

Paritala, S., Singaram, K. K., Bathina, I., Khan, M. A., and Jyosyula, S. K. R. (2023). Rheology and pumpability of mix suitable for extrusion-based concrete 3D printing–A review. *Constr. Build. Mater.* 402, 132962. doi:10.1016/j.conbuildmat.2023.132962

Park, C. K., Noh, M. H., and Park, T. H. (2005). Rheological properties of cementitious materials containing mineral admixtures. *Cem. Concr. Res.* 35 (5), 842–849. doi:10.1016/j.cemconres.2004.11.002

Ramzi, S., and Hajiloo, H. (2023). The effects of supplementary cementitious materials (SCMs) on the residual mechanical properties of concrete after exposure to high temperatures—review. *Buildings* 13 (1), 103. doi:10.3390/buildings13010103

Riaz, M., Alam, Z., Zafar, T., Javed, U., and Akhlaq, H. (2022). Investigation of mechanical and durability properties of sustainable high-strength concrete. *Proc. Inst. Civ. Eng. - Forensic Eng.* 176 (1), 3–15. doi:10.1680/jfoen.22.00008

Roussel, N. (2006). A thixotropy model for fresh fluid concretes: theory, validation and applications. *Cem. Concr. Res.* 36 (10), 1797–1806. doi:10.1016/j.cemconres.2006.05.025

Roussel, N., Lemaître, A., Flatt, R. J., and Coussot, P. (2010). Steady state flow of cement suspensions: a micromechanical state of the art. *Cem. Concr. Res.* 40 (1), 77–84. doi:10.1016/j.cemconres.2009.08.026

Roy, D. M. (1982). Hydration, structure, and properties of blast furnace slag cements, mortars, and concrete. *J. Proc.* 79 (6), 444–457.

Rumman, R. (2018). Mix design for durable and pumpable concrete using locally available materials.

Samad, S., and Shah, A. (2017). Role of binary cement including Supplementary Cementitious Material (SCM), in production of environmentally sustainable concrete: a critical review. *Int. J. Sustain. Built Environ.* 6 (2), 663–674. doi:10.1016/j.ijsbe.2017.07.003

Sankar, B., and Ramadoss, P. (2022). "Mechanical and durability properties of high strength concrete incorporating different combinations of supplementary cementitious materials: a review," in *Proceedings of fourth international conference on inventive material science applications: ICIMA 2021*, 543–557.

Siddique, R. (2014). Utilization of industrial by-products in concrete. *Procedia Eng.* 95, 335–347. doi:10.1016/j.proeng.2014.12.192

Siddique, R., and Bennacer, R. (2012). Use of iron and steel industry by-product (GGBS) in cement paste and mortar. *Resour. Conserv. Recycl.* 69, 29–34. doi:10.1016/j.resconrec.2012.09.002

Standard, A. C. I. (1996). Standard practice for selecting proportions for normal, heavyweight, and mass concrete. *ACI Man. Concr. Pr.* 1996, 1–38.

Stanmore, B. R., and Gilot, P. (2005). Review—calcination and carbonation of limestone during thermal cycling for CO2 sequestration. *Fuel Process. Technol.* 86 (16), 1707–1743. doi:10.1016/j.fuproc.2005.01.023

Sun, Y., Wang, Z., Park, D., Kim, W., Kim, H., Yan, S., et al. (2022). Analysis of the isothermal hydration heat of cement paste containing mechanically activated fly ash. *Thermochim. Acta* 715, 179273. doi:10.1016/j.tca.2022.179273

Suresh, D., and Nagaraju, K. (2015). Ground granulated blast slag (GGBS) in concrete–a review. *IOSR J. Mech. Civ. Eng.* 12 (4), 76–82. doi:10.9790/1684-12467682

Taerwe, L., and Matthys, S. (2013). *Fib model code for concrete structures 2010*. Ernst & Sohn, Wiley.

Venkitasamy, V., Santhanam, M., Rao, B. P. C., Balakrishnan, S., and Kumar, A. (2024). Mechanical and durability properties of structural grade heavy weight concrete with fly ash and slag. *Cem. Concr. Compos.* 145, 105362. doi:10.1016/j.cemconcomp.2023.105362

Vikan, H., and Justnes, H. (2007). Rheology of cementitious paste with silica fume or limestone. *Cem. Concr. Res.* 37 (11), 1512–1517. doi:10.1016/j.cemconres.2007.08.012

Wan, H., Shui, Z., and Lin, Z. (2004). Analysis of geometric characteristics of GGBS particles and their influences on cement properties. *Cem. Concr. Res.* 34 (1), 133–137. doi:10.1016/s0008-8846(03)00252-7

Yu, H., Yi, Y., and Unluer, C. (2021). Heat of hydration, bleeding, viscosity, setting of Ca (OH) 2-GGBS and MgO-GGBS grouts. *Constr. Build. Mater.* 270, 121839. doi:10.1016/j.conbuildmat.2020.121839

Yuan, Q., Shi, C., and Jiao, D. (2022). *Rheology of fresh cement-based materials: fundamentals, measurements, and applications*. London, United Kingdom: CRC Press.